Comparison of the quasifree charge-exchange reaction for ^{12}C and ^{54}Fe

K. H. Hicks,[1] W. P. Alford,[2] A. Celler,[2,3] R. S. Henderson,[4,5] K. P. Jackson,[4] C. A. Miller,[4] M. C. Vetterli,[4] S. Yen,[4] F. Brieva,[6] C. J. Horowitz,[7] and J. Piekarewicz[8]

[1] *Department of Physics, Ohio University, Athens, Ohio 45701*
[2] *University of Western Ontario, London, Ontario, Canada, N6A 3K7*
[3] *Simon Fraser University, Burnaby, British Columbia, Canada, V5A 1S6*
[4] *TRIUMF, 4004 Wesbrook Mall, Vancouver, British Columbia, Canada, V6T 2A3*
[5] *University of Melbourne, Melbourne, Australia*
[6] *University of Chile, Casilla 487-3, Santiago, Chile*
[7] *Indiana University, Bloomington, Indiana 47405*
[8] *Florida State University, Tallahassee, Florida 32306*

(Received 29 July 1992)

The $(\vec{p}, n)$ reaction has been measured for ^{12}C and ^{54}Fe targets at 290 MeV for a laboratory angle of 20.4° and at 420 MeV for a laboratory angle of 24.0°. This paper presents new cross section data and analyzing powers at excitation energies near the quasifree peak. The data are compared with recently developed nonrelativistic calculations and with extended relativistic calculations that include random phase approximation correlations.

PACS number(s): 25.40.Kv, 24.70.+s

I. INTRODUCTION

A typical energy spectrum for a proton scattered from the nucleus has discrete peaks at low energy loss followed by a broad continuum known as the quasifree region. It is generally believed that this continuum results from nucleon knockout, with both scattered and knockout nucleons sharing the incident energy. Indeed, the quasifree region exhibits a peak close to the energy expected from kinematics of nucleon-nucleon (NN) scattering at the same momentum transfer. When both free NN scattering from a hydrogen target and quasifree nucleon knockout from a nuclear target exhibit the same kinematics, then differences in the observables can help one's understanding of how the nuclear medium modifies the NN interaction. A comparison of the analyzing powers from NN scattering with the analyzing power at the quasifree peak gives an indication of these "medium modifications."

The width of the quasifree peak is reasonably described by simple models of Fermi motion [1] of the knockout nucleon. Nuclear structure will also contribute at some level since the nucleon can be knocked out from any of the nuclear shells occupied in the ground state. However, knockout from shell states near the surface of the nucleus is preferred because the incoming nucleon interacts strongly with nuclear matter. As a result, most calculations of the observables for the quasifree region use a surface-response model [2] or calculate transmission coefficients using an eikonal approximation [3]. Although the strongest medium modification effects are expected for nucleons near the center of the nucleus, these surface-localized calculations still predict large effects on the observables, particularly for the analyzing power, in the quasifree region [3].

Nuclear structure is usually assumed to play a minimal role in the quasifree region. The knockout nucleon can come from any of the nuclear shell states into the continuum, and so the quasifree observables will average over all contributions thereby obscuring nuclear structure effects. However, the influence of giant resonances, which lie at excitation energies just above the discrete nuclear transitions, can affect the cross section and spin observables. The data in the giant resonance region are in reasonable agreement with nuclear structure effects calculated using the random phase approximation (RPA) [4, 5]. In order to avoid these complications, measurements of the quasifree region are usually done at larger angles where the quasifree peak is kinematically shifted away from the giant resonance region.

Many of the results reported for observables in the quasifree region have used the $(\vec{p}, p')$ reaction at intermediate energies (100 to 800 MeV). At these incident proton energies the central (non-spin-flip) part of the NN interaction reaches its minimum strength, which allows the proton to probe deeper into the nucleus. At 500 MeV, the spin observables for ^{12}C are measured to be nearly the same as the free NN spin observables [6], except for the polarization which is suppressed by about 30%. At other energies and with other targets, similar results are seen [7]. For example, data [4] from the $^{54}Fe(\vec{p}, p')$ reaction at 290 MeV show both the analyzing power A_y and the polarization P to be below the values calculated by a nonrelativistic surface response model by a factor of 2. Relativistic calculations [8] (using the Dirac equation) predict a suppression of A_y by 30 to 50 %. The suggestion has been made [8] that this may be the clearest "relativistic" signature found to date. The mechanism for the suppression of the analyzing power in relativistic calculations is directly related to the large and opposing vector

and scalar potentials usually assumed in these models [8]. However, an alternative explanation emerges from a recently developed nonrelativistic model [9] which includes the nonlocal couplings in the nuclear response and the full off-shell behavior of the internucleon force. This model shows some suppression of A_y for the (p,p') data, depending on the off-shell force used, although definitive calculations are not yet available.

The $(\vec{p},p')$ reaction in the quasifree region is expected to proceed mainly via the exchange of mesons with neutral charge, such as the ω or the π^0, or through two-pion exchange (usually represented by σ-meson exchange). At energies above approximately 300 MeV, the contributions from other mesons through so-called exchange diagrams is expected to be small [8]. The present work reports cross sections and analyzing powers in the quasifree region for the $(\vec{p},n)$ reaction at 290 and 420 MeV. The $(\vec{p},n)$ reaction was chosen because it is expected to proceed via the exchange of charged mesons, such as the $\pi^{\pm}$ and $\rho^{\pm}$. Here, the effect of the nuclear medium is expected to be quite different since, in contrast to the $(\vec{p},p')$ reaction to which both isoscalar and isovector transitions contribute, the $(\vec{p},n)$ reaction is purely isovector. Data from the $(\vec{p},n)$ reaction are a good test of the predictions from relativistic model calculations. Alternatively, we can assess the importance of nonlocal couplings and off-shell effects in the nonrelativistic framework.

One of the most interesting results from the previous $(\vec{p},n)$ quasifree measurements [10] was the comparison of the ^{12}C and ^{54}Fe analyzing powers. In contrast to the $(\vec{p},p')$ measurements where A_y is suppressed by about 30% or more independent of the target or beam energy [7], the A_y for $(\vec{p},n)$ measurements were seen [10] to be suppressed for ^{12}C yet *enhanced* for ^{54}Fe at excitation energies below the quasifree peak. The present results, with a completely new data set, confirm these observations, and extend the measurements past the quasifree peak. Cross section data for the quasifree peak are presented for the first time at these incident proton energies.

II. EXPERIMENTAL DETAILS

The data were collected at TRIUMF using the large angle charge-exchange configuration in the proton hall. Figure 1 shows a schematic of this setup. A proton beam strikes the target of interest, producing neutrons which strike a liquid scintillator and produce recoil protons of nearly the same energy. The recoil protons are momentum analyzed in the medium resolution spectrometer (MRS) consisting of a quadrupole-dipole combination [11]. The primary proton beam continues to the beam dump where the beam current is monitored by a secondary-electron emission monitor. Protons from the $(\vec{p},p')$ reaction are either blocked (at large angles) by iron and lead shielding or are bent to smaller angles by a small dipole magnet placed between the target and the recoil scintillator. A thin plastic scintillator was placed just before the recoil scintillator in order to veto any protons or neutral atomic hydrogen that pass through the dipole. The recoil scintillator rates were typically 0.2 to

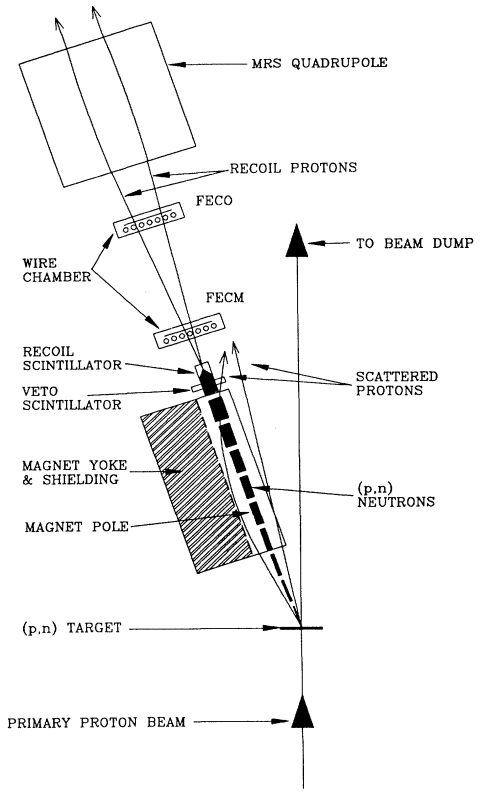

FIG. 1. Schematic layout of the large-angle charge-exchange configuration using the medium resolution spectrometer (MRS) at TRIUMF.

0.6 MHz, and the veto scintillator rates were an order of magnitude lower.

The recoil scintillator dimensions were 2.54 cm by 2.54 cm in the horizontal plane and 6.0 cm vertically. It was placed 80 cm from the target. The scintillator material was BC513 with a density of 0.735 g/cm^2 and a C to H ratio of 1:2. Neutrons striking the hydrogen in the scintillator at forward angles will transfer essentially their full energy to the proton. Protons from the (n,p) reaction on carbon will contaminate the spectrum, but this can be eliminated as described in the next section. The recoil protons pass through two sets of front end chambers (FEC0 and FECM), each with horizontal and vertical wire planes, which allow tracking back to the recoil scintillator. Typical front-end chamber rates were about 100 kHz. Software cuts were made to eliminate protons originating outside of the scintillator volume. The spectrometer solid angle for detection of the recoil proton was typically 2.1 msr. The light output from the recoil scintillator was used to correct the energy loss of the recoil proton, giving a final energy resolution of about 1.5 MeV.

The beam polarization was monitored continuously using an in-beam polarimeter (IBP) consisting of a thin (1.37 mg/cm^2) CH_2 target and plastic scintillators set at conjugate angles appropriate for proton-proton elastic scattering. The IBP also served as a monitor of the beam current. Typical beam polarizations were 77% at

290 MeV and 70% at 420 MeV, and typical beam currents were 100 nA. The computer deadtime was measured by counting the number of triggers generated and the number read by the computer, with typical livetimes of 96%. This may be compared with the previous data [10] where the system was run harder with livetimes of about 85%. The wire-chamber efficiencies were calculated using the redundancy built into the wire-chamber planes, with typical efficiencies of all eight planes together of between 70 and 80 %.

III. DATA ANALYSIS

The normalizations of the cross sections were determined from the integrated beam charge, the target thickness, the proton recoil efficiency (calculated using the NN phase shifts for forward angle neutron-proton scattering), the spectrometer solid angle (measured from the front-end wire-chamber tracking), the livetime, and the detector efficiency. A ^{7}Li target was used to check the normalization, and the resulting cross sections were in good agreement with previously measured values [12] with a statistical error of 6%. The target thicknesses were 285.5 mg/cm^2 for ^{12}C, 196.4 mg/cm^2 for ^{54}Fe, and 115 mg/cm^2 for ^{7}Li. An energy calibration was obtained by using the ^{7}Li$(p,n)^7$Be ground plus first excited state peak and the ^{12}C$(p,n)^{12}$N 4^- stretched state at 4.52 MeV.

The MRS has a momentum bite of $\Delta p/p \simeq 10\%$, but the acceptance is not uniform across the whole range. The acceptance has been measured previously [13] by scanning the ^{7}Li ground-state peak across the focal plane by varying the MRS magnet settings. The resulting cross sections were fit with a smooth function of the focal-plane position. The fit is nearly flat for most of the momentum bite, and falls off sharply at either end. A cut was made on the flat part of the acceptance, resulting in corrections of only a few percent. The data were taken in two separate momentum bites for both the 290 and 420 MeV energies.

A correction is also needed for the C(n,p)N reaction in the recoil scintillator. This was accomplished by using the measured C(n,p)N spectrum [13, 14] at 300 and 460 MeV. These energies are close to the 290 and 420 MeV energies of the present measurements. The main contribution in the subtraction is from the nearly constant C(n,p)N continuum, so the uncertainty in energy matching is assumed to be negligible. However, the C(n,p)N subtraction is a cumulative effect, as shown by a figure in Ref. [10], and makes up to a 30% correction at the highest energy losses measured here. In addition, the momentum bite measured here is larger than the measured C(n,p)N spectrum, so it was necessary to artificially extend the spectrum an extra 20 MeV beyond the measured C(n,p)N continuum. This gives additional uncertainty to the shape of the quasifree cross section at the higher energy losses and in particular to the location of the quasifree peak. Nonetheless, this correction is a smooth function of energy loss ω and the quasifree peak centroid can still be ascertained to within a few MeV.

IV. DISCUSSION

A. Model calculations

The calculations that are compared with the data in the following figures are from two models. One is a relativistic RPA calculation of the nuclear matter response [15], shown by solid curves below. The other calculation, which is shown by a dashed curve, is a nonrelativistic finite nucleus calculation[9] based on a local density approximation to the nuclear response and including nonlocal couplings and off-shell effects of the nucleon-nucleon effective interaction. For comparison, a dotted line corresponding to the free scattering value of A_y as given by NN phase shifts [16] is also shown.

The relativistic plane-wave impulse approximation calculations were done with the projectile described by Dirac spinors with masses shifted from their free value by the strong scalar potential [8]. The projectile interacted with the medium via the isovector part of the t matrix parametrized from on-shell data in a Lorentz invariant way. The linear response of the nuclear ground state was then calculated in a random phase approximation. The isovector correlations in the medium were generated by an isovector pion and a ρ meson containing both vector and tensor couplings to the nucleon with the parameters obtained from the Bonn one-boson exchange potential. Finally, the effect of short-range correlations was simulated by including Landau-Migdal parameters having values of $g'_\pi = 0.6$ for the pion and $g'_\rho = 0.3$ for the ρ meson.

The relativistic calculation gives a higher value of A_y than does the phase-shift solutions, due to the effective mass terms for the pseudovector coupling, as described in Ref. [8]. We use effective mass values of $M^*/M = 0.84$ for ^{12}C and $M^*/M = 0.80$ for ^{54}Fe. Pseudovector coupling is generally preferred over pseudoscalar coupling from considerations of elastic scattering and chiral invariance [17]. Earlier work [10] emphasized the simpler pseudoscalar coupling. The relativistic calculations, in the absence of RPA correlations, reduce to the NN scattering value (from phase shift solutions) at the quasifree peak for values of $M^*/M = 1.0$.

The nonrelativistic calculations correspond to a parameter free model [9] and the predicted results have not been normalized. This model relies on the energy-dependent Franey-Love effective nucleon-nucleon interaction [18] and on an interacting Fermi-gas model [19] to calculate the unperturbed nuclear response and the distorting nucleon-nucleus optical potential in a local density approximation. The distorted incoming and outgoing nucleon scattering wave functions are calculated in the eikonal approximation [2, 9]. Furthermore, shell effects accounting for the reaction Q value and the target recoil are also considered [20]. This is important in order to predict the position of the quasielastic peak.

B. Data at 420 MeV

The cross section and analyzing powers for the ^{12}C$(\vec{p},n)$ reaction at 420 MeV are shown in Fig. 2 at

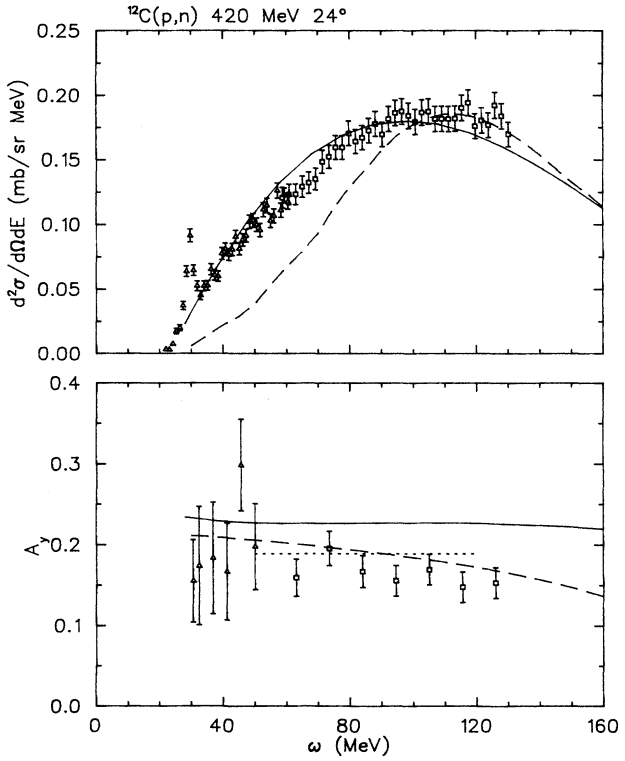

FIG. 2. Cross section and analyzing power for the reaction shown as a function of the measured energy loss ω. The solid line is from a relativistic model calculation [15] and the dashed curve is from a nonrelativistic model [9]. The free NN scattering value is shown by the dotted line.

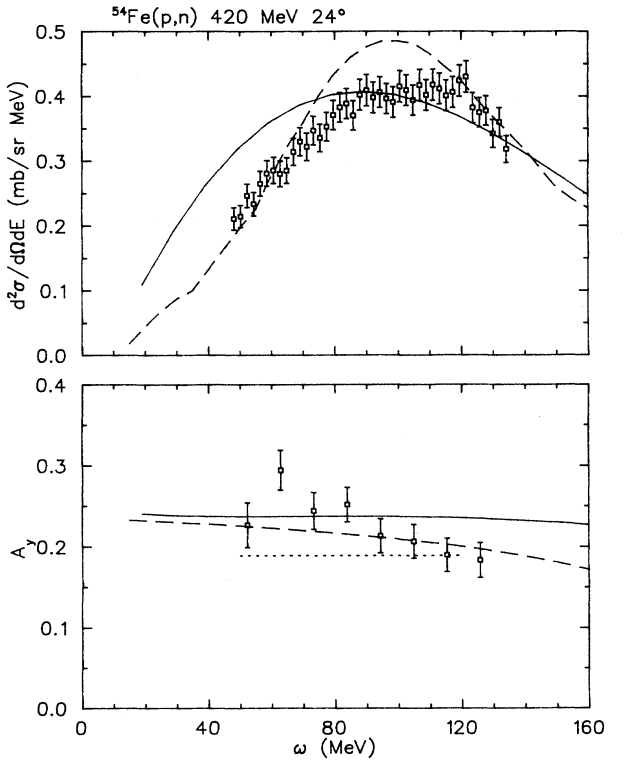

FIG. 3. See caption to Fig. 2.

24°, and in Fig. 3 for the ^{54}Fe$(\vec{p},n)$ reaction at the same energy and angle. The relativistic calculations in Fig. 2 have been shifted up by the Q value of the reaction. This is a nontrivial point, since one is not guaranteed that the residual nucleus is left intact. Comparing the Q value for a nucleon knockout reaction such as ^{12}C$(p,np)^{11}$C, which has $Q = -16.5$ MeV, with the Q value for the ^{12}C$(p,n)^{12}$B reaction at $Q = -18.1$ MeV, there is not a large difference. The relativistic model calculations in Fig. 2 have been shifted up in ω by 18 MeV, and similarly in Fig. 3 where the shift is 9 MeV for the Q value of the ^{54}Fe$(p,n)^{54}$Co reaction. Again, we emphasize that these shifts applied to the solid curves are rough approximations since the calculations assume a zero Q value. In addition, the relativistic model calculations must be normalized by the effective number of nucleons $A_{\rm eff}$ that participate in the reaction. The solid curves shown in Figs. 2 and 3 use $A_{\rm eff} = 3.4$ and $A_{\rm eff} = 8.2$, respectively. These values are close to those calculated in Ref. [8]; exact calculations for $A_{\rm eff}$ require good elastic scattering data.

The predicted cross section from the nonrelativistic model is in fair agreement with the ^{12}C data. However, this model fails to explain the correct width for the quasielastic peak. For the ^{54}Fe cross sections, where the absorption effects are more difficult to estimate accurately, the agreement is still within 20%. Systematic errors in the data normalization are dominated by the energy scale calibration (note that cross section *per MeV* are plotted) and are expected to be less than 8%. Systematic errors for the A_y data are dominated by the calibration of the in-beam polarimeter, which is known to be less than 2%.

The A_y data for ^{12}C in Fig. 2 are shown for both low and high momentum bites of the spectrometer. The A_y data below $\omega = 60$ MeV are too low for comparison with the calculations, since these data are too far away from the quasifree peak. Near the quasifree peak, the A_y data are slightly below both the nonrelativistic calculations and the free scattering value. The data are significantly below the prediction from the relativistic calculation with pseudovector coupling. Shown in Fig. 3 are the A_y data for ^{54}Fe which are close to both calculations at the quasifree peak, but move above these calculations at lower excitation energy. In contrast to the ^{12}C data, the ^{54}Fe data are slightly above the free scattering value at the quasifree peak. It is interesting that at $\omega = 120$ MeV, the A_y data for both nuclei agree (within errors) but at $\omega = 60$ MeV, the strong slope to the ^{54}Fe data moves it above the ^{12}C data. The difference between ^{12}C and ^{54}Fe at low ω is an indication that nuclear structure cannot be ignored so far away from the quasifree peak even at the large momentum transfer given here ($q = 2.05$ fm^{-1}).

One other analyzing power measurement in the quasifree region has been published for the ^{12}C$(\vec{p},n)$ reaction at 495 and 795 MeV [21] They find the analyzing power for ^{12}C at 495 MeV to be consistent with the free NN scattering value of A_y at the quasifree peak. Their

measurement also finds the A_y data for a ^{40}Ca target to be slightly above the free value at the quasifree peak and rising at smaller ω, consistent with the A_y data for the ^{54}Fe target of the present results.

The cross sections at 420 MeV display a broad peak with centroids at an energy loss of 110 ± 5 MeV for both ^{12}C and ^{54}Fe targets. This is what would be expected for in-medium NN scattering, where the very different binding energies for ^{12}C ($Q = -18.1$ MeV) and ^{54}Fe ($Q = -9.0$ MeV) become unimportant. For comparison, the cross section shapes for ^{12}C (solid line) and ^{54}Fe (dotted line) are plotted in Fig. 4. The ^{12}C data has been multiplied by the ratio $(54/12)^{2/3}$ as expected for a surface-dominated reaction mechanism. The cross section data for both nuclei follow roughly the same shape. This close correspondence in shape is also seen in the raw data, as shown in Fig. 5. At the quasifree peak, the A_y for both nuclei are also in reasonable agreement. These are indications that the inclusive (p,n) reaction mechanism at 420 MeV incident proton energy is dominated by the quasifree process for values of ω near the quasifree peak.

C. Data at 290 MeV

The data for ^{12}C and ^{54}Fe at 290 MeV and an angle of 20.4° are shown in Figs. 6 and 7. The relativistic calculations in these figures have the same Q value shifts as were used in Figs. 2 and 3. As with the 420 MeV A_y data, the 290 MeV A_y data for ^{54}Fe again have a steeper slope than for the 290 MeV ^{12}C data. The A_y data generally fall between the calculations, although at the quasifree peak the data are in better agreement with the nonrelativistic prediction. Also, the ^{12}C data are in good agreement with the free scattering value of A_y. In contrast, the ^{54}Fe data in Fig. 7 agree with the free scattering value at the quasifree peak, but move upward for lower ω. Since this trend is seen at both energies, this

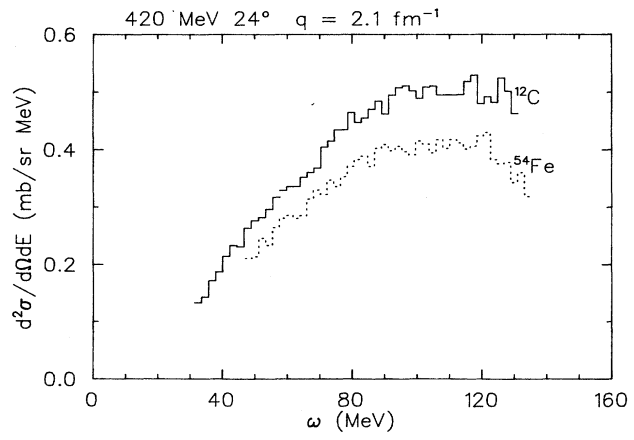

FIG. 4. Comparison of the cross section shape for ^{12}C and ^{54}Fe cross sections at 420 MeV. The ^{12}C target data (solid) has been multiplied by a factor of $(54/12)^{2/3}$ as described in the text.

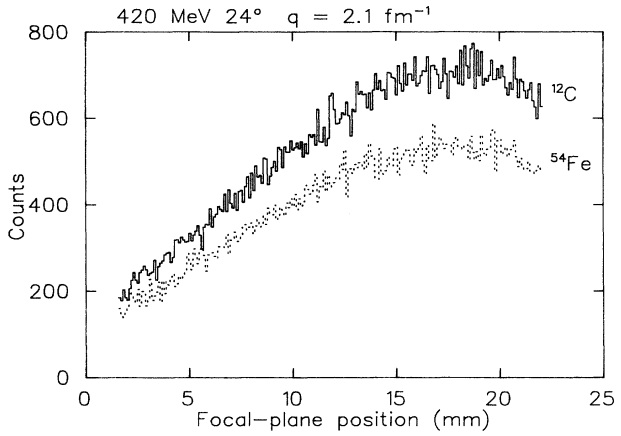

FIG. 5. The raw data, before corrections for the acceptance and for the C(n,p)N component in the recoil scintillator.

reinforces the interpretation that nuclear structure becomes increasingly important at energy losses somewhat below the quasifree peak.

The cross sections for ^{12}C and ^{54}Fe at 290 MeV are seen to peak at energy losses of 68 ± 8 and 80 ± 10 MeV, respectively. In contrast, the results at 420 MeV showed the quasifree peak at the same energy loss for both nuclei. The relativistic calculations in Figs. 6 and 7 have been normalized with $A_{\text{eff}} = 2.9$ and $A_{\text{eff}} = 6.0$ for ^{12}C and

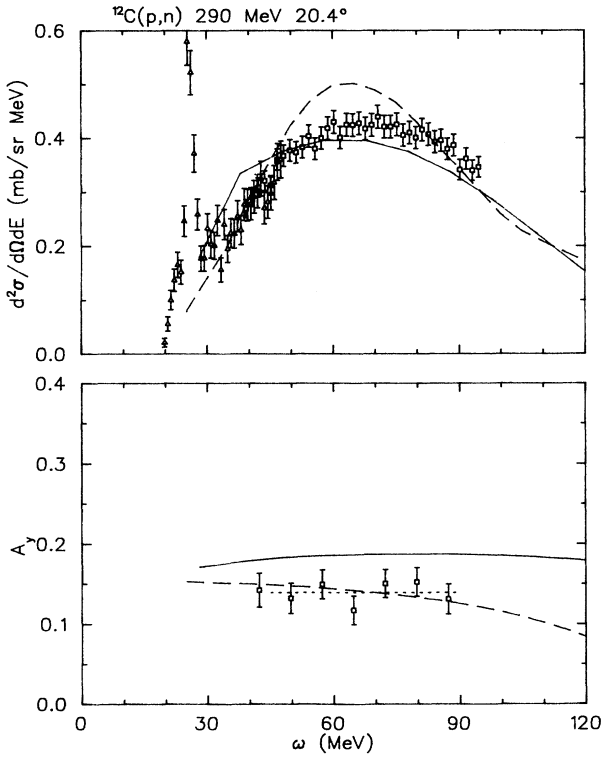

FIG. 6. See caption to Fig. 2.

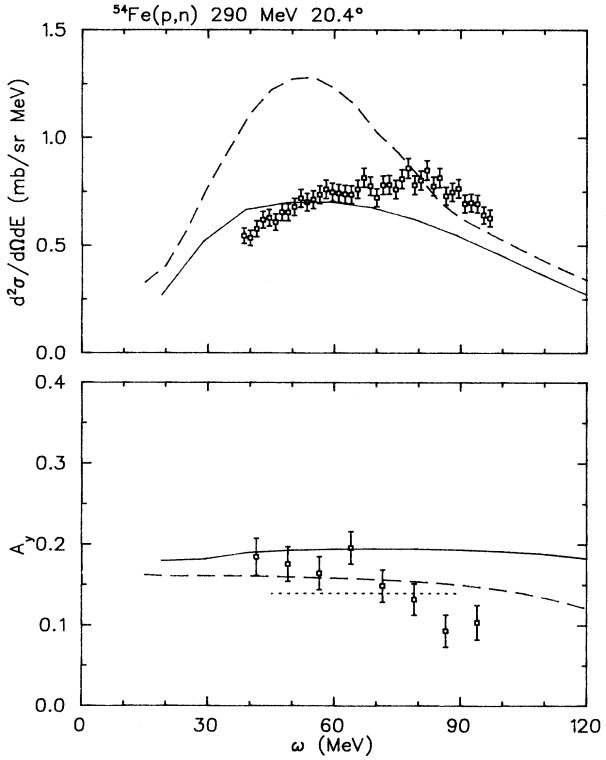

FIG. 7. See caption to Fig. 2.

^{54}Fe, respectively. The nonrelativistic calculations are not modified by any normalization. For the ^{12}C data, neither calculation is in good agreement with the cross section, although the peak position for the nonrelativistic calculation is reasonably close to the peak of the data. For the ^{54}Fe data, both models fail to agree with the cross section data. The most interesting discrepancy is the position of the quasielastic peak which experimentally comes at a higher energy loss than expected. There is no simple explanation for this feature in the context of simple quasifree scattering from either the relativistic or the nonrelativistic models.

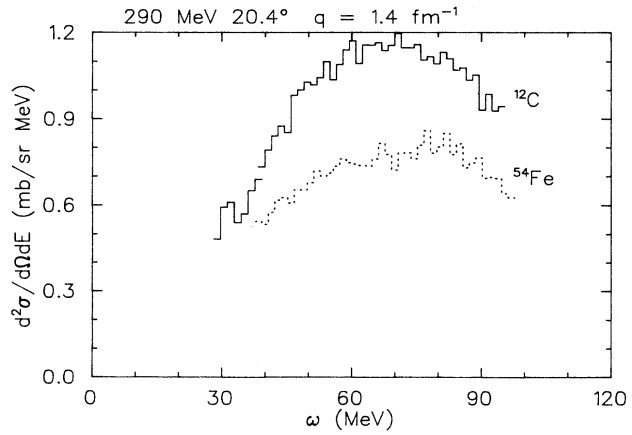

FIG. 8. See caption to Fig. 4.

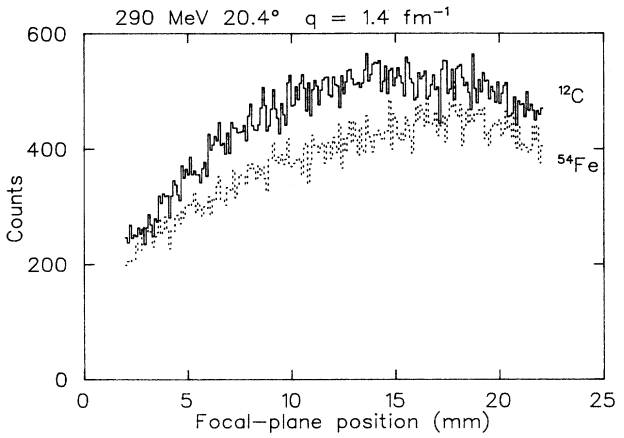

FIG. 9. See caption to Fig. 5.

For comparison, the cross section data for both nuclei are plotted in Fig. 8, where again the ^{12}C data has been multiplied by the ratio $(54/12)^{2/3}$. Direct comparison of the cross section data for ^{12}C and ^{54}Fe give different values for ω at the quasifree peak. The different shapes for the ^{12}C and ^{54}Fe data are also clearly seen in the raw data, before any corrections have been applied, as shown in Fig. 9. The 290 MeV data in Fig. 9 can be contrasted with the 420 MeV data shown in Fig. 5, where the shapes for ^{12}C and for ^{54}Fe are roughly the same. The data for both nuclei were acquired in adjacent runs, with identical settings of the spectrometer and of the beam tune, at both 290 and 420 MeV.

The ratio of cross section for ^{12}C and ^{54}Fe at the quasifree peak, as shown in Fig. 8 at 290 MeV, is further away from the $A^{2/3}$ scaling expected for surface-dominated scattering. Both of these features point to effects other than pure quasifree scattering. Indeed, the multistep contributions are expected to be more important in heavier targets at lower energies. It has also been suggested [22], based on $(e, e'p)$ data, that multinucleon knockout makes a significant contribution at excitation energies above the quasifree peak. These multistep and multinucleon knockout contributions are a plausible explanation for the nonquasifree features of the data, although no calculations are available at present to test this conjecture.

The peak at 4.5 MeV in the cross section data for the ^{12}C target is due to a direct reaction exciting states with a J^π of 2^- and 4^-. This conglomerate has been previously studied with the (e, e') reaction [23] and the (n, p) reaction [24]. The cross section is dominated by the 4^- stretched state at momentum transfers $q > 1.6$ fm^{-1}. For completeness, we have extracted cross sections for this peak in the center-of-mass frame of 0.95 ± 0.15 mb/sr at 290 MeV ($q = 1.40$ fm^{-1}), and 0.16 ± 0.02 mb/sr at 420 MeV ($q = 2.05$ fm^{-1}).

V. SUMMARY AND CONCLUSIONS

The present data support previous results that the A_y data for ^{12}C$(\vec{p}, n)$ at 420 MeV follow a different trend in

energy loss ω than for ^{54}Fe$(\vec{p},n)$ at the same angle and beam energy. At the quasifree peak, the A_y data for ^{12}C and ^{54}Fe are close to the free NN scattering value of A_y at both 290 and 420 MeV. At both incident proton energies, the A_y data for ^{54}Fe is more steeply sloped in ω than the ^{12}C data, suggesting the importance of structure effects below the quasifree peak.

New cross section data at 290 and 420 MeV were presented. The cross section data at 420 MeV for both ^{12}C and ^{54}Fe peak at approximately the same value of ω, but at 290 MeV, the cross section data for ^{54}Fe peaks about 10 MeV higher in the energy loss ω. Also, the ratio of cross sections for ^{12}C and ^{54}Fe at the quasifree peak is only 2.0 for the 290 MeV data set, whereas the 420 MeV data are closer to the expected ratio of 2.7 for a surface-dominated reaction mechanism such as nucleon knockout. Both the peak location and the Fe/C ratio suggest that the 420 MeV data exhibit trends closer to the quasifree process than do the 290 MeV data. This may be due to the onset of multistep and multinucleon knockout contributions at the lower energy.

The data were compared with new nonrelativistic calculations, based on the Franey-Love force and a local density description of the nuclear response, and with new relativistic calculations using a pseudovector coupling with RPA correlations. The predictions from the relativistic model were shifted to higher energy loss based on kinematics calculations. The A_y data generally fall between the relativistic and nonrelativistic calculations, but are in better agreement with the nonrelativistic predictions at values of ω near the quasifree peak. The relativistic model, which is successful in predicting the $\sim$30% suppression of A_y for the $(\vec{p},p')$ reaction, does not properly describe the present $(\vec{p},n)$ data, at least for calculations using the present pseudovector coupling. On the other hand, the nonrelativistic calculations that are in rough agreement with the A_y from the present data do not properly describe the A_y for the $(\vec{p},p')$ reaction in the quasifree region. Further theoretical investigation is needed to understand how to correctly describe the spin observables, particularly the analyzing power, for both the (p,n) and (p,p') reactions in the quasifree region.

ACKNOWLEDGMENTS

We thank Jack Rapaport for many enlightening discussions. Communications with Terry Taddeucci were also very helpful. The work of the TRIUMF technical staff is also gratefully acknowledged. This work was supported in part by Grant PHY-9112739 from the National Science Foundation. F.B. acknowledges Grant 1239-90 from FONDECYT.

[1] H. Esbensen and G. Bertsch, Phys. Rev. C **34**, 1419 (1986).
[2] R.D. Smith, in *Spin Observables of Nuclear Probes*, Proceedings of the 4th Telluride International Conference, edited by C.J. Horowitz, C.D. Goodman, and G.E. Walker (Plenum, New York, 1988), p. 15.
[3] C.J. Horowitz and M.J. Iqbal, Phys. Rev. C **33**, 2059 (1986).
[4] O. Häusser *et al.*, Phys. Rev. C **43**, 230 (1991).
[5] F.T. Baker *et al.*, Phys. Rev. C **44**, 93 (1991).
[6] T. Carey *et al.*, Phys. Rev. Lett. **53**, 144 (1984).
[7] K.H. Hicks, in *Intersections Between Nuclear and Particle Physics*, Proceedings of a Conference held in Rockport, ME, edited by G.M. Bunce, AIP Conf. Proc. No. 176 (AIP, New York, 1988), p. 26.
[8] C.J. Horowitz and D.P. Murdock, Phys. Rev. C **37**, 2032 (1988).
[9] F.A. Brieva and W.G. Love, Phys. Rev. C **42**, 2573 (1990).
[10] K.H. Hicks *et al.*, Phys. Rev. C **40**, 2445 (1989).
[11] C.A. Miller, TRIUMF Report No. TRI-83-3, p. 339.
[12] J.W. Watson *et al.*, Phys. Rev. C **40**, 22 (1989).
[13] M.C. Vetterli *et al.*, Phys. Rev. C **40**, 559 (1989).
[14] A. Trudel, private communication.
[15] J. Piekarewicz and C.J. Horowitz, Florida State Report FSU-SCRI-92-135. See also C.J. Horowitz and J. Piekarewicz, Nucl. Phys. **A511**, 461 (1990).
[16] R.A. Arndt and L.S. Roper, code SAID with FA91 phase-shift solutions (unpublished).
[17] D.P. Murdock and C.J. Horowitz, Phys. Rev. C **35**, 1442 (1987).
[18] M.A. Franey and W.G. Love, Phys. Rev. C **31**, 488 (1985).
[19] C. Alvarez, M.Sc. thesis, University of Chile, 1990; C. Alvarez, F.A. Brieva, W.G. Love, and K. Nakayama, Phys. Rev. C **46**, 565 (1992).
[20] F. Brieva and J. Rapaport, private communication.
[21] T.N. Tadduecci, in *Spin and Isospin in Nuclear Interactions*, Proceedings of the 5th Telluride International Conference, edited by S.W. Wissink, C.D. Goodman, and G.E. Walker (Plenum, New York, 1991), p. 393; T.N. Taddeucci *et al.*, Nucl. Phys. **A527**, 393c (1991).
[22] W. Bertozzi, in Proceedings of the 1992 CEBAF Summer Workshop (AIP, New York, in press).
[23] R.S. Hicks, J.B. Flanz, R.A. Lindgren, G.A. Peterson, L.W. Fagg, and D.J. Millener, Phys. Rev. C **30**, 1 (1984).
[24] R. Pourang, Ph.D. thesis, Kent State University, 1991; B.D. Anderson *et al.*, Phys. Rev. C **46**, R504 (1992).